DOI: 10.1002/ejic.201000944

Cp*⁻-Ruthenium–Nickel-Based H_2-Evolving Electrocatalysts as Bio-inspired Models of NiFe Hydrogenases

Sigolène Canaguier,[a] Marc Fontecave,[a,b] and Vincent Artero*[a]

Keywords: Hydrogen / Biomimetic synthesis / Enzyme models / Metalloenzyme models / Electrocatalysis / Nickel / Ruthenium

Three dinuclear nickel–ruthenium complexes [Ni(xbsms)-RuCp*(L)](PF_6) [H_2xbsms = 1,2-bis(4-mercapto-3,3-dimethyl-2-thiabutyl)benzene; Cp* = pentamethylcyclopentadienyl; L = CH_3CN, CO and O_2] are reported that act as bio-inspired mimics of NiFe hydrogenases. Because of an increased electron density at the metal centres in comparison with the previously described [Ni(xbsms)RuCp(L)](PF_6) (Cp = cyclopentadienyl) analogues, these compounds catalyze the evolution of hydrogen from Et_3NH^+ in DMF with an overpotential reduced by around 50 mV, thereby corroborating a previously established structure–function relationship [*Eur. J. Inorg. Chem.* **2007**, *18*, 2613–2626; *Chem. Eur. J.* **2009**, *15*, 9350–9364]. In addition, the steric protection provided by the bulky Cp*⁻ ligand results in an increased catalytic rate and stability upon cycling.

Introduction

Hydrogenases are metalloenzymes found in micro-organisms that employ hydrogen as an energy source or release it as a byproduct of metabolism.[1] These fascinating natural molecular catalysts have been shown to compete with platinum in terms of electrocatalytic properties for the interconversion of H_2 with $2H^+$ and $2e^-$.[2] Interestingly, their active sites (Figure 1) do not contain any noble metal but cheap and available nickel and iron. Therefore they are a valuable source of inspiration for the design of original electrocatalysts as mid- or long-term alternatives to the use of platinum in H_2-related technological devices.[3] A great variety of synthetic diiron complexes have been reported as structural models of the active site of FeFe hydrogenases and are also catalytically competent for the reduction of protons to H_2 in non-aqueous media.[4] In contrast, and despite the synthesis of more than 50 structural mimics of the active site of NiFe hydrogenases, only two dinuclear Ni–Fe complexes with significant catalytic activity have been reported.[5,6] In parallel, a series of nickel-based catalysts for the evolution of hydrogen in which Ru replaces Fe have been described by the group of Ogo and co-workers[7–9] for the oxidation of H_2 and by our group for the evolution of H_2.[10–12] Complexes with {Ni(μ-SR)$_2$Ru(CO)$_2$Cl$_2$},[10,12,13] {Ni(μ-SR)$_2$Ru(arene)Cl}[10] or {Ni(μ-SR)$_2$RuCpL} (Cp = cyclopentadienyl, L = DMSO or CO)[11] structures display electrocatalytic activity for the reduction of protons from Et_3NH^+ in DMF. A key parameter for evaluating H_2-evolving electrocatalysts is the determination of the overpotential, which is the extra energy required for the redox reaction in comparison with that strictly required thermodynamically; this is a measure of the energy lost in the reaction. The overpotential is defined as the difference between the potential needed to be applied to the system to make it function at a significant rate and the standard potential of the redox couple. Until now, and even though they contain a biologically non-relevant noble metal atom, the Ni–Ru systems appear to be better electrocatalysts than the above-mentioned Ni–Fe compounds because they catalyse the evolution of H_2 with lower overpotentials. A comparison of the catalytic performances of this series has allowed a structure–function relationship to be derived: the overpotential for the evolution of hydrogen decreases as the electron density at the dinuclear metal centre increases.[10] It was thus tempting to further investigate this trend and to

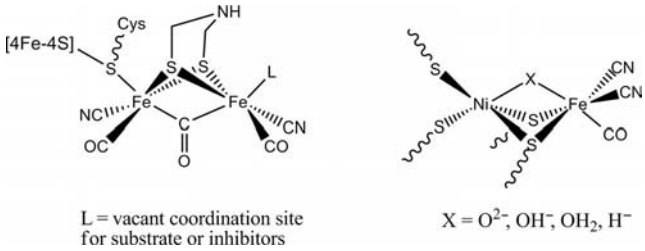

Figure 1. Structures of the active sites of iron-only hydrogenases in the oxidized state (left) and NiFe hydrogenases (right) in the oxidized Ni–B inactive ready state (X = O^{2-}, OH^- or H_2O) or reduced Ni–C active state (X = H^-).[1]

[a] Laboratoire de Chimie et Biologie des Métaux, Université Grenoble 1, CNRS UMR 5249, CEA DSV/iRTSV, 17 rue des Martyrs, 38054 Grenoble Cedex 9, France
Fax: +33-4-38789124
E-mail: vincent.artero@cea.fr
[b] Collège de France, 11 place Marcellin-Berthelot, 75005 Paris, France

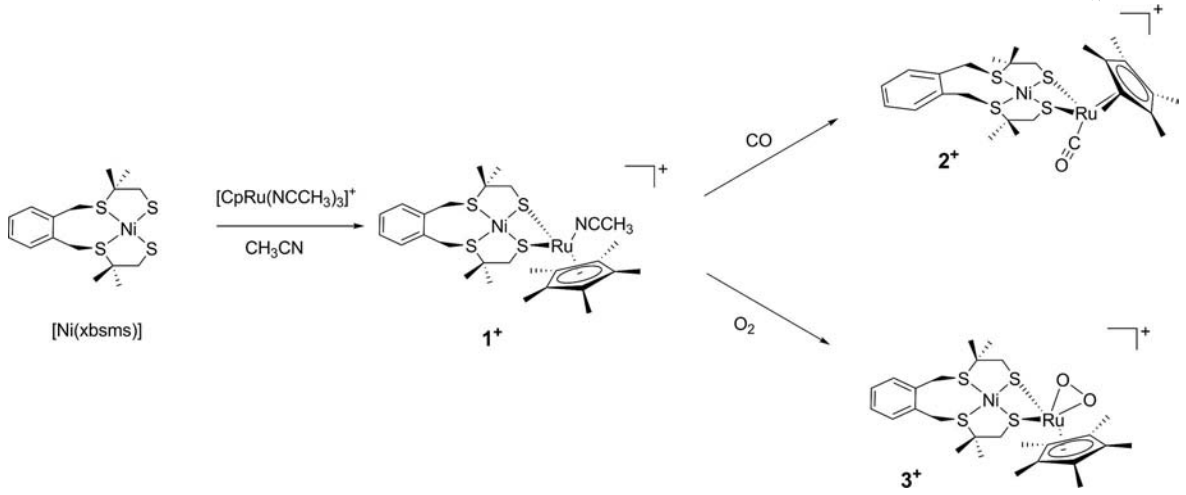

Scheme 1. Synthesis of **1**(PF_6), **2**(PF_6) and **3**(PF_6).

substitute a more electron-rich organometallic moiety, such as the pentamethylcyclopentadienylruthenium $\{RuCp^*\}^+$ fragment, for the $\{RuCp\}^+$ centre present in the best Ni–Ru catalyst described so far.[11] We report in this paper the preparation of three new {Ni(xbsms)RuCp*} [H_2xbsms = 1,2-bis(4-mercapto-3,3-dimethyl-2-thiabutyl)benzene] compounds (Scheme 1). As expected from the above structure–reactivity relationship and due to the cumulative inductive effect of the five methyl substituents, the Cp^{*-} ligand provides the {Ni(xbsms)Ru} framework with an overpotential around 50 mV lower for the evolution of H_2 than those previously reported for Cp^--containing Ni–Ru complexes. Increased stabilities are also observed.

Results

Synthesis and Characterization

Reaction of [Ni(xbsms)][14] with commercial $[Cp^*Ru(CH_3CN)_3](PF_6)$ in CH_3CN readily affords a blue-green compound that reacts very rapidly with molecular oxygen. This has so far prevented its structural characterization. Monomeric dinuclear $[Ni(xbsms)RuCp^*(CH_3CN)](PF_6)$ or dimeric tetranuclear $[\{Ni(xbsms)RuCp^*\}_2](PF_6)_2$ structures can be proposed for this compound by analogy with Cp*Ru–Ni compounds with different ligands around the nickel centre described by Rauchfuss and co-workers.[15] The ^{1}H NMR spectrum of this compound displays a singlet assigned to the equivalent protons of the Cp^{*-} ligand, one singlet for the methyl groups of the $xbsms^{2-}$ ligand and two broad signals corresponding to the benzylic and methylenic protons of the $xbsms^{2-}$ ligand. Such a pattern is not consistent with a rigid tetranuclear structure that should display two AB systems for the benzylic and methylenic protons and distinct signals for the equatorial and axial methyl groups of the $xbsms^{2-}$ ligand. Instead, the ^{1}H NMR spectrum can be explained by the presence in solution of two isomers of a stereochemically non-rigid dinuclear compound of formula $[Ni(xbsms)RuCp^*(CH_3CN)](PF_6)$ [**1**(PF_6), Scheme 1]. Such a stereochemical non-rigidity has already been observed in two other Ni–Ru and Ni–Fe compounds in the series.[6,11]

Compound [Ni(xbsms)RuCp*(CO)](PF_6) [**2**(PF_6), Scheme 1] was formed rapidly when **1**(PF_6) was stirred in CH_3CN under CO, as revealed by electrospray ionisation mass spectrometry with a molecular peak observed at *m*/*z* = 667 and by infrared spectroscopy with a band assigned to the stretching mode of the carbonyl ligand observed at 1921 cm^{-1}. This value is 24 cm^{-1} lower than that observed for the Cp analogue [Ni(xbsms)RuCp(CO)](PF_6), which indicates that the introduction of the Cp* ligand increases the electron density at the ruthenium centre. The ^{1}H NMR spectrum indicates that **2**(PF_6) exists in solution as a single isomer with C_s symmetry and heterotopic faces. Small monocrystals could be obtained from the diffusion of diethyl ether vapour into a CH_3CN solution of **2**(PF_6). Although the quality of the diffraction data recorded was not good enough to obtain a satisfactory model, their analysis allowed us to conclude that this compound possesses the same structural arrangement (shown in Scheme 1) as the related Cp^- compound [Ni(xbsms)RuCp(CO)](PF_6).[11]

When handled out of the glove-box, solutions of **1**(PF_6) rapidly turned brown. The ^{1}H NMR spectrum of the black material obtained after removal of the solvent shows the presence of only one compound with C_s symmetry. The mass spectrum reveals the addition of an O_2 ligand to the cationic $\{Ni(xbsms)RuCp^*\}^+$ framework. All of these data are consistent with the formation of $[Ni(xbsms)RuCp(O_2)](PF_6)$ with molecular oxygen coordinated side-on to the ruthenium centre as previously reported by Rauchfuss and co-workers for a comparable Ni–Ru compound.[15]

Electrochemical Properties

Cyclic voltammograms of compounds **1**(PF_6)–**3**(PF_6) were recorded at a glassy carbon electrode in DMF with n-Bu_4NBF_4 as the supporting electrolyte. Compound **1**(PF_6) shows two irreversible cathodic monoelectronic waves lo-

cated at –1.00 and –1.34 V versus Ag/AgCl (Figure 2). By analogy with the Cp analogues,[11] the irreversibility of the first process has been attributed to the elimination of the CH_3CN ligand from the coordination sphere of Ru upon reduction. Complex **2**(PF_6) experiences a reversible one-electron reduction at –0.86 V versus Ag/AgCl (ΔE_p = 120 mV; $i_{pa}/i_{pc} \approx 1$) followed by an irreversible cathodic wave at –1.50 V versus Ag/AgCl (Figure 3). The cyclic voltammogram of **3**(PF_6) displays two main and poorly resolved irreversible cathodic waves between –0.6 and –0.8 V versus Ag/AgCl (Figure 4). Small cathodic signals are also

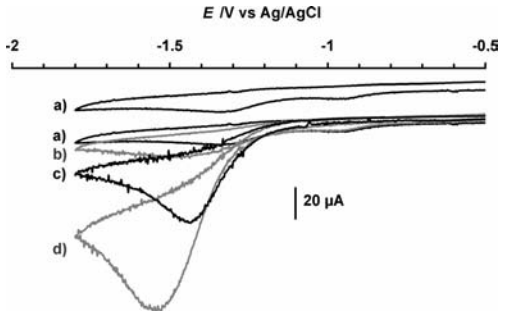

Figure 2. Cyclic voltammograms of **1**(PF_6) (1.0 mmol L^{-1}) in the absence (a, shown twice) and in the presence of various amounts of Et_3NHCl recorded in a DMF solution of nBu_4NBF_4 (0.1 mol L^{-1}) at a glassy carbon electrode at 100 mV s^{-1}. b) 1.5, c) 5.0 and d) 10 equiv. of Et_3NHCl. The rather high noise is due to the specific set-up used to record electrochemical data in the glovebox.

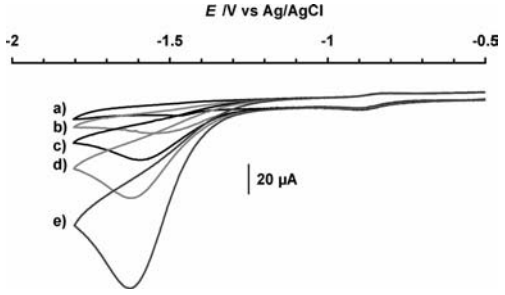

Figure 3. Cyclic voltammograms of **2**(PF_6) (1.0 mmol L^{-1}) in the presence of various amounts of Et_3NHCl recorded in a DMF solution of nBu_4NBF_4 (0.1 mol L^{-1}) at a glassy carbon electrode at 100 mV s^{-1}.a) 0, b) 1.0, c) 3.0, d) 5.0 and e) 10 equiv. of Et_3NHCl.

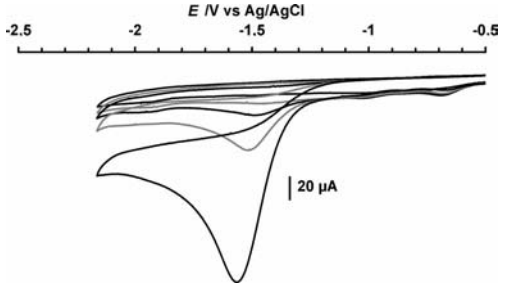

Figure 4. Cyclic voltammograms of **3**(PF_6) (1.0 mmol L^{-1}) in the presence of various amounts of Et_3NHCl recorded in a DMF solution of nBu_4NBF_4 (0.1 mol L^{-1}) at a glassy carbon electrode at 100 mV s^{-1}. Top-down: 0, 1.0, 3.0, 5.0 and 10 equiv. of Et_3NHCl.

observed at –1.0 and –1.3 V that have been tentatively assigned to the reduction of $\mathbf{1}^+$. We propose that the latter species is formed as the product of the reductive processes observed between –0.6 and –0.8 V versus Ag/AgCl maybe through the release of a peroxo or hydroperoxo ligand.

Electrocatalytic Evolution of Hydrogen in the Presence of Et_3NH^+

Figure 2 shows the cyclic voltammogram of compound **1**(PF_6) measured in DMF at a glassy carbon electrode. Upon addition of triethylammonium chloride a cathodic catalytic wave is observed at –1.40 V versus Ag/AgCl. This wave is the only noticeable modification of the cathodic part of the cyclic voltammogram of **1**(PF_6). The intensity i_c of this new wave increases with the number of added equivalents of Et_3NH^+, as shown by the evolution of the i_c/i_p ratio (with i_p the peak intensity of a monoelectronic wave in the voltammogram recorded in the absence of acid, Figure 5), which measures the catalytic current enhancement. These features are typical of an electrocatalytic process that converts Et_3NH^+ into H_2. When **2**(PF_6) was used as the electrocatalyst under the same conditions, hydrogen was evolved at –1.60 V versus Ag/AgCl (Figure 3). The reversible process at –0.86 V versus Ag/AgCl remained unchanged. This behaviour is very similar to that of the Cp analogue but, as evidenced in Figure 5, the catalytic current enhancement is significantly higher for **2**(PF_6) than for [Ni(xbsms)RuCp(CO)](PF_6). Finally, **3**(PF_6) catalyses the evolution of H_2 with a catalytic current enhancement similar to **1**(PF_6) but at a significantly lower potential (–1.52 V vs. Ag/AgCl, Figure 4).

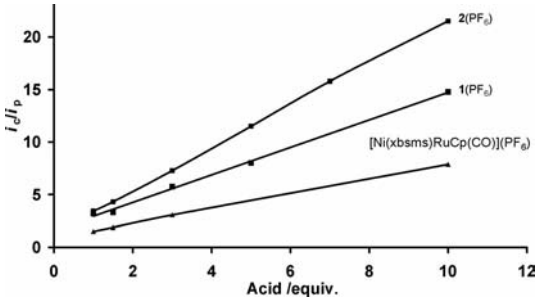

Figure 5. Evolution of the i_c/i_p ratio between the catalytic peak current and the current of a monoelectronic wave as a function of the number of added equivalents of Et_3NHCl for **1**(PF_6), **2**(PF_6) and [Ni(xbsms)RuCp(CO)](PF_6).

Bulk Electrolysis Experiments

When **1**(PF_6) was used as the electrocatalyst during the bulk electrolysis of Et_3NHCl at a mercury pool electrode at –1.60 V versus Ag/AgCl in DMF, more than 36 turnovers were achieved within 5 h, which corresponds to a conversion of around 75% of Et_3NHCl into H_2, detected as the sole gas produced during the reaction.

Table 1. Electrocatalytic properties of **1**(PF_6), **2**(PF_6), previously reported Ni–Ru catalysts[11] and mononuclear precursors.[a]

	E_{her}[b] [V] (1.5 equiv.)	E_{her}[b] [V] (3 equiv.)	E_{her}[b] [V] (10 equiv.)	Total TON[c] (after 3 h)	TOF[c] [h^{-1}]	TOF_0[d] [h^{-1}]
1(PF_6)	–1.44	–1.40	–1.53	27.8	9.3	11.1
2(PF_6)	–1.54	–1.60	–1.63	6.6	2.2	2.9
[Ni(xbsms)RuCp(dmso)](PF_6)	–1.39	–1.44	–1.48	13	4.3	7
[Ni(xbsms)RuCp(CO)](PF_6)	–1.60	–1.65	–1.61	15.8	5.3	6.7
[Ni(xbsms)]	–1.45	–1.46	–1.52	5.1	1.7	2.3
[Cp*Ru(CH_3CN)$_3$](PF_6)	–1.56	–1.41	–1.66	5.1	1.7	1.8

[a] All potentials are quoted vs. Ag/AgCl. [b] The electrocatalytic peak potentials (E_{her}) were determined in the presence of 3 equiv. of acid by cyclic voltammetry at 100 mV s^{-1} in a DMF solution of nBu_4NBF_4 (0.1 mol L^{-1}) at a glassy carbon electrode. [c] TOF and total TON were determined by bulk electrolysis experiments at –1.60 V vs. Ag/AgCl in a DMF solution (7 mL) of nBu_4NBF_4 (0.1 mol L^{-1}) and Et_3NHCl (0.5 mmol) at a mercury pool (1.23 cm^2) in the presence of millimolar concentrations of catalyst. [d] Initial turnover frequency (TOF_0) corresponds to the number of cycles achieved during the first hour of electrolysis.

Discussion

Table 1 reports the measured electrocatalytic parameters for compounds **1**(PF_6) and **2**(PF_6) and compares them with those of previously reported H_2-evolving Ni–Ru electrocatalysts containing the Cp^- ligand bound to ruthenium.[11] From these data, we can easily determine the overpotentials for the evolution of hydrogen displayed by these new catalysts. For a better comparison with previously reported catalysts of the Ni–Ru series, we used in this work the same method for the determination of the overpotential as in our previous research: we calculated the difference between the tabulated value of the standard potential of the Et_3NH^+/H_2 couple in DMF (–0.78 V vs. Ag/AgCl) and the peak potentials of the catalytic waves measured in the presence of 3 equiv. of Et_3NH^+. It is found that **1**(PF_6) and **2**(PF_6) catalyse the evolution of H_2 with overpotentials 40 to 50 mV lower than the corresponding Cp analogues [Ni(xbsms)-RuCp(dmso)](PF_6) and [Ni(xbsms)RuCp(CO)](PF_6),[16] as expected from the previously established structure–function relationship.[10] Hence, with an overvoltage for H_2 evolution of 620 mV, **1**(PF_6) appears to be the most efficient dinuclear mimic of the active site of NiFe hydrogenase described so far. We previously noted that the CO-coordinated complex [Ni(xbsms)RuCp(CO)](PF_6) displays significantly higher overpotentials than the solvent-coordinated catalyst [Ni(xbsms)RuCp(dmso)](PF_6). The same observation is made on comparison of the catalytic properties of **1**(PF_6) and **2**(PF_6). We proposed that these two classes feature distinct catalytic mechanisms for the evolution of H_2.[11]

In addition, and unexpectedly, the presence of the Cp^{*-} ligand also has a significant effect on the rate of catalysis for which the catalytic current enhancement i_c/i_p can be used as a proxy (Figure 5). Both **1**(PF_6) and **2**(PF_6) display higher rates of catalysis than their corresponding Cp analogues.[11] This effect is not likely to arise from any electronic effect introduced by the substitution of the Cp^{*-} for the Cp^- ligand. Indeed it has been observed in two series of H_2-evolving catalysts[17,18] that any electronic modification at the catalytic centre that lowers the overpotential for the evolution of H_2 also leads to a decrease in the rate of catalysis. We thus attribute this improvement of the catalytic rate in the new series to the steric effect of the bulky Cp^{*-} ligand that protects the catalytic centre from any deactivation processes during turnover.

Table 1 also allows a comparison with the results obtained from bulk electrolysis experiments with compounds **1**(PF_6) and **2**(PF_6) and other previously reported H_2-evolving Ni–Ru electrocatalysts under identical experimental conditions. Complex **1**(PF_6) appears to be the most efficient catalyst among the {Ni(xbsms)} series as far as turnover frequency is concerned. Remarkably, its rate of catalysis is almost fully sustained during the 3 h experiment, whereas the Cp analogue becomes significantly inactivated under similar conditions. Here again, this gain in stability is likely due to the steric protection of the active centre of the catalyst provided by the bulky Cp^{*-} ligand. In contrast, **2**(PF_6) shows poor performances under bulk electrolysis conditions although a high stability, similar to that of its Cp analogue, is observed during the experiment. For the sake of comparison, we performed bulk electrolysis experiments on the whole Ni–Ru series at –1.60 V versus Ag/AgCl. As a consequence, in the case of **2**(PF_6), the high catalytic current enhancement observed by cyclic voltammetry is balanced by a driving force for electrocatalytic hydrogen evolution that is around 200 mV lower than for **1**(PF_6).

Conclusions

As a result of a combination of electronic and steric effects, the introduction of a Cp^{*-} ligand into the coordination sphere of the ruthenium centre has led to the preparation of [Ni(xbsms)RuCp*(CH_3CN)]$^+$, the most active and robust bio-inspired Ni–Ru catalyst known so far for the evolution of hydrogen. The improvement not only concerns the overpotential for the evolution of H_2, reduced by around 50 mV, but also the catalytic rates and stability upon cycling. In addition, the exposure of [Ni(xbsms)-RuCp*(CH_3CN)]$^+$ to air yields an O_2 adduct that is still catalytically active towards the evolution of hydrogen under reductive conditions. This system may thus be considered as a model for the reductive activation of the inactive (Ni-A or Ni-B) forms of the NiFe hydrogenases.

Experimental Section

Materials: All reactions were routinely performed under argon using standard Schlenk techniques. Specifically, the synthesis of **1**(PF_6) was carried out in a glove-box. Solvents were degassed and distilled under argon. Diethyl ether was distilled by heating at reflux over Na/benzophenone and dry dichloromethane was obtained by distillation on CaH_2. NMR solvents (Eurisotop) were deoxygenated by three freeze–pump–thaw cycles and stored over molecular sieves. Commercial dimethylformamide for use in the electrochemical experiments was degassed by bubbling nitrogen through it. [Ni(xbsms)] was prepared according to a previously reported procedure.[14] [Cp*Ru(CH_3CN)$_3$](PF_6) was purchased from Strem Chemicals and used without further purification. The supporting electrolyte ($n$$Bu_4N$)$BF_4$ was prepared from ($n$$Bu_4N$)$HSO_4$ (Aldrich) and $NaBF_4$ (Aldrich) and dried overnight at 80 °C under vacuum. Triethylammonium chloride (Acros) and CO (Air Liquide) were used as received.

Methods and Instrumentation: NMR spectra were recorded at room temperature in 5-mm tubes with a Bruker AC 300 spectrometer equipped with a QNP probehead operating at 300.0 MHz for ^{1}H NMR. Solvent peaks were used as internal references relative to Me_4Si for ^{1}H NMR chemical shifts (listed in ppm). ESI mass spectra were recorded with a Finnigan LCQ thermoquest ion-trap spectrometer. Elemental analyses were performed at the Service Central d'Analyse du CNRS (Vernaison, France). All electrochemical measurements were carried out under nitrogen at room temperature. A standard three-electrode configuration was used consisting of a glassy carbon (3 mm in diameter) or platinum (2 mm in diameter) disk as the working electrode, an auxiliary platinum wire and an Ag/AgCl/aqueous $AgCl_{sat}$ + KCl 3 M (given as Ag/AgCl throughout this text) reference electrode closed by a Vycor frit and dipped directly into the solution. To take into account the liquid junction potential between aqueous and non-aqueous solutions, this electrode was calibrated with the internal reference system Fc^+/Fc, which was found at 0.53 V versus Ag/AgCl in dimethylformamide. The Fc^+/Fc couple (E_0 = 0.400 V vs. SHE)[19] was used to quote potentials relative to a SHE when needed. Cyclic voltammograms were recorded with an EG&G PAR 273M instrument for the catalyst and 0.1 M for the supporting electrolyte ($n$$Bu_4N$)$BF_4$. Electrodes were polished with an MD-Nap polishing pad with a 1 μm monocrystalline diamond DP suspension and DP lubricant blue (Struers). Et_3NHCl was added by syringe as a 50 mM solution in dimethylformamide. Blank cyclic voltammograms of the supporting electrolyte and of Et_3NHCl in DMF may be found in previous reports.[20] Bulk electrolysis experiments and coulometry were performed with an EG&G PAR 273A instrument in DMF using a mercury pool cathode. The platinum-grid counter electrode was placed in a separate compartment connected by a glass frit and filled with a 0.1 M solution of ($n$$Bu_4N$)$BF_4$ in degassed dimethylformamide. A made-to-measure electrolysis cell with a cylindrical reservoir was used. The mercury pool surface was therefore identical from one experiment to another. The mercury surface was measured as 1.23 cm^2 and the electrolysis cell constant was determined to be 2.34×10^{-4} s^{-1} by performing bulk electrolysis of methylviologen hexafluorophosphate.[10] The following procedure was followed for catalytic acid reduction bulk electrolysis: a degassed DMF solution (7 mL) containing 0.1 M ($n$$Bu_4N$)$BF_4$ and the acid (0.1 M) was first electrolysed at the desired potential until the current reached 1% of its initial value. The catalyst (1 mM) was then added and electrolysis was performed at the same potential and monitored by coulometry. The purity of the hydrogen was tested with a Delsi Nermag DN200 GC chromatograph equipped with a 3 m Porapack column and a thermal conductivity detector (TCD). Nitrogen at a pressure below 1 bar was used as the carrier gas. The whole apparatus was thermostatted at 45 °C. Under these conditions, pure hydrogen had an elution time of 77 s.

Synthesis of [Ni(xbsms)RuCp*(CH_3CN)](PF_6) [1(PF_6)]: [Ni(xbsms)] (20 mg, 0.050 mmol) and [Cp*Ru(CH_3CN)$_3$](PF_6) (25 mg, 0.050 mmol) were dissolved in CH_3CN (8 mL) and the blue-green solution was stirred for 20 min. After filtration, the solvent was removed in vacuo and the resulting blue-green powder (36 mg, 88%) was washed with diethyl ether. Due to the high sensitivity of this compound to air, no reliable elemental analysis could be obtained. ^{1}H NMR (CD_3CN): δ = 7.35 (m, 4 H, Ar), 4.34 (m, 4 H, $ArCH_{ax}H_{eq}S$), 3.70 [m, 4 H, $(CH_3)_2CCH_{eq}H_{ax}$], 1.95 (s, 12 H, Me), 1.68 (s, 15 H, Cp*) ppm. UV/Vis (CH_3CN): λ_{max} (ε) = 332 (sh, 3300), 400 (sh, 1600), 638 (1200 $M^{-1}cm^{-1}$) nm.

Synthesis of [Ni(xbsms)RuCp*(CO)](PF_6) [2(PF_6)]: [Ni(xbsms)] (76 mg, 0.189 mmol) and [Cp*Ru(CH_3CN)$_3$](PF_6) (97 mg, 0.192 mmol) were dissolved in CH_3CN (15 mL) and the solution was stirred for 20 min under 2 bar of CO atmosphere. The mixture turned from blue-green to brown. The solution obtained was filtered and the solvents evaporated to dryness. The product was then washed with diethyl ether and dried (136 mg, 89%). ^{1}H NMR ([D_6]DMSO): δ = 7.42 (m, 4 H, Ar), 5.94 (m, 2 H, $ArCH_{ax}H_{eq}S$), 4.28 (m, 2 H, $ArCH_{eq}H_{ax}S$), 2.72 [m, 2 H, $(CH_3)_2CCH_{eq}H_{ax}$], 1.99 [m, 2 H, $(CH_3)_2CCH_{eq}H_{ax}$], 1.75 (s, 15 H, Cp*), 1.70 (s, 6 H, Me_{ax}), 1.61 (s, 6 H, Me_{eq}) ppm. ^{13}C NMR (CD_3CN): δ = 202.20 (M–*C*O), 134.91, 132.35, 130.96 (Ar), 97.55 (C_5Me_5), 56.13 [*C*(CH_3)$_2$], 34.75 [C(CH_3)$_2$*C*H_2S], 26.35 (Ar*C*H_2S), 10.15 [CH_3, C_5(*C*H_3)$_5$] ppm. IR (KBr): $\tilde{\nu}$ = 1921 (CO stretching vibration) cm^{-1}. MS (ESI): *m*/*z* (%) = 667 (100) $[M]^+$, 639 (35) $[M - CO]^+$. UV/Vis (CH_3CN): λ_{max} (ε) = 397 (sh, 1000), 516(sh, 400 $M^{-1}cm^{-1}$) nm. $C_{27}H_{39}F_6NiOPRuS_4$ (812.59): calcd. C 39.91, H 4.84, S 15.78; found C 39.12, H 4.74, S 13,31.

Synthesis of [Ni(xbsms)RuCp*(O_2)](PF_6) [3(PF_6)]: [Ni(xbsms)] (66 mg, 0.164 mmol) and [Cp*Ru(CH_3CN)$_3$](PF_6) (82 mg, 0.164 mmol) were dissolved in degassed CH_3CN (15 mL) and stirred in air for 20 min. The blue-green solution immediately turned brown. The solution obtained was filtered and the solvents evaporated to dryness. The black product was then washed with diethyl ether and dried (83 mg, 65%). ^{1}H NMR (CD_2Cl_2): δ = 7.33 (m, 4 H, Ar), 5.60 (d, J_{AB} = 12.6 Hz, 2 H, $ArCH_{ax}H_{eq}S$), 3.66 (d, J_{AB} = 12.6 Hz, 2 H, $ArCH_{eq}H_{ax}S$), 3.09 [d, J_{AB} = 12.6 Hz, 2 H, $(CH_3)_2CCH_{eq}H_{ax}$], 2.05 [d, J_{AB} = 12.6 Hz, 2 H, $(CH_3)_2CCH_{eq}H_{ax}$], 1.84 (s, 6 H, Me_{ax}), 1.60 (s, 15 H, Cp*), 1.56 (s, 6 H, Me_{eq}) ppm. MS (ESI): *m*/*z* (%) = 671 (100) $[M]^+$, 639 (90) $[M - O_2]^+$. UV/Vis (CH_3CN): λ_{max} (ε) = 332 (sh, 3200), 433 (sh, 600), 607 (100 $M^{-1}cm^{-1}$) nm. $C_{26}H_{39}F_6NiO_2PRuS_4$ (816.57): C 38.24, H 4.81, F 13.96, Ni 7.19, P 3.79, Ru 12.38, S 15.71; found C 38.86, H 5.04, F 13.18, Ni 6.58, P 4.07, Ru 12.40, S 14.50.

Acknowledgments

The authors thank Colette Lebrun of the Laboratoire de Reconnaissance Ionique et Chimie de Coordination of the SCIB (UMR UJF/CEA-E3) for ESI-MS analysis. This work was supported by the BioHydrogen program of the Life Science Division of CEA and the French National Research Agency (ANR, grant number 07-BLAN-0298-01)

[1] J. C. Fontecilla-Camps, A. Volbeda, C. Cavazza, Y. Nicolet, *Chem. Rev.* **2007**, *107*, 4273–4303.

[2] A. K. Jones, E. Sillery, S. P. J. Albracht, F. A. Armstrong, *Chem. Commun.* **2002**, 866–867.
[3] S. Canaguier, V. Artero, M. Fontecave, *Dalton Trans.* **2008**, 315–325.
[4] C. Tard, C. J. Pickett, *Chem. Rev.* **2009**, *109*, 2245–2274.
[5] B. E. Barton, C. M. Whaley, T. B. Rauchfuss, D. L. Gray, *J. Am. Chem. Soc.* **2009**, *131*, 6942–6943.
[6] S. Canaguier, M. Field, Y. Oudart, J. Pécaut, M. Fontecave, V. Artero, *Chem. Commun.* **2010**, *46*, 5876–5878.
[7] S. Ogo, R. Kabe, K. Uehara, B. Kure, T. Nishimura, S. C. Menon, R. Harada, S. Fukuzumi, Y. Higuchi, T. Ohhara, T. Tamada, R. Kuroki, *Science* **2007**, *316*, 585–587.
[8] B. Kure, T. Matsumoto, K. Ichikawa, S. Fukuzumi, Y. Higuchi, T. Yagi, S. Ogo, *Dalton Trans.* **2008**, 4747–4755.
[9] T. Matsumoto, B. Kure, S. Ogo, *Chem. Lett.* **2008**, *37*, 970–971.
[10] Y. Oudart, V. Artero, J. Pécaut, C. Lebrun, M. Fontecave, *Eur. J. Inorg. Chem.* **2007**, 2613–2626.
[11] S. Canaguier, L. Vaccaro, V. Artero, R. Ostermann, J. Pécaut, M. Field, M. Fontecave, *Chem. Eur. J.* **2009**, *15*, 9350–9365.
[12] L. Vaccaro, V. Artero, S. Canaguier, M. Fontecave, J. M. Field, *Dalton Trans.* **2010**, *39*, 3043–3049.
[13] Y. Oudart, V. Artero, J. Pécaut, M. Fontecave, *Inorg. Chem.* **2006**, *45*, 4334–4336.
[14] J. A. W. Verhagen, D. D. Ellis, M. Lutz, A. L. Spek, E. Bouwman, *J. Chem. Soc., Dalton Trans.* **2002**, 1275–1280.
[15] M. A. Reynolds, T. B. Rauchfuss, S. R. Wilson, *Organometallics* **2003**, *22*, 1619–1625.
[16] Comparison between the CH_3CN and DMSO adducts is fully licit here because these ligands are likely eliminated from the Ru coordination sphere during the first reductive event.
[17] R. M. Kellett, T. G. Spiro, *Inorg. Chem.* **1985**, *24*, 2373–2377.
[18] X. Hu, B. S. Brunschwig, J. C. Peters, *J. Am. Chem. Soc.* **2007**, *129*, 8988–8998.
[19] H. M. Koepp, H. Wedt, H. Strehlow, *Z. Elektrochem.* **1960**, *64*, 483.
[20] M. Razavet, V. Artero, M. Fontecave, *Inorg. Chem.* **2005**, *44*, 4786–4795.

Received: September 5, 2010
Published Online: December 12, 2010

